Supplementary Materials

Colorful Aerogel Fibers Enabling Functional Textiles for Thermal Insulation and Harmful-Gas Visualization

Peiqi Liu[a], Xinya Zheng[a], Yajie Shu[a], Yongming Cui[a], Yirong Wang[d,e], Jinming Zhang[c,*], Jinfeng Wang[a,*], Jun Zhang[c], Xungai Wang[b]

[a] Wuhan Textile University, National Local Joint Laboratory for Advanced Textile Processing and Clean Production, Wuhan 430200, China

[b] College of Textile Science and Engineering, Zhejiang SCI-TECH University, Hangzhou 310016，China

[c] CAS Key Laboratory of Engineering Plastics, Institute of Chemistry, Chinese Academy of Sciences (CAS), Beijing, 100190, China

[d] Key Laboratory of Major Hazard Sources and System Safety of Chemical Industry Park, Ministry of Emergency Management of China, Beijing 100012, China

[e] China Academy of Safety Science and Technology, Beijing 100012, China

EXPERIMENTAL SECTION

Materials

Cotton fibers used in this study were provided by Shuangli Medical Supplies Co., Ltd. Polyvinylamine (MW = 502.31) were purchased from Aladdin Reagent Co., Ltd., China. Dimethyl sulfoxide, methyl red, bromothymol blue, and bromophenol blue were obtained from Shanghai Macklin Biochemical Technology Co., Ltd. 1-Butyl-3-methylimidazolium acetate was acquired from Qingdao Aolike New Materials Technology Co., Ltd. Glutaraldehyde (25% aqueous solution), citric acid, sodium hydroxide, sodium bisulfate, pararosaniline hydrochloride, acetic acid, ammonia solution, formaldehyde, methanol, acetone, and absolute ethanol were provided by China Pharmaceutical Chemical Reagent Co., Ltd. Deionized water was used for all the experiments.

Preparation of amino-modified cotton cellulose (CE@PEI)

Cotton fiber (1 g) was dissolved in 50 mL of 8% NaOH solution and soaked at 5 °C for 5 hrs. After washing, 30 mL of 2.7% PEI solution was added dropwise, and the mixture was stirred at 50 °C for 3 hrs. Subsequently, the solution was cooled to room temperature, and 1 mL of glutaraldehyde was added, followed by stirring for 2 hrs. The mixture was then filtered and repeatedly washed with water until neutral pH. The washed sample was dried in a fume hood to a constant weight to obtain amino-functionalized cotton fiber sample (CE@PEI).

Preparation of cellulose aerogel fiber (CE-aerogel fiber)

Cotton fibers (0.28 g) were dissolved in a mixed solution of 1.6 g ionic liquid [BMIM][OAc](ILs) and 6.4 g dimethyl sulfoxide (DMSO) under magnetic stirring at 45 °C until complete dissolution. The spinning solution was extruded through wet-spinning. The obtained fibers were subsequently transferred to a water bath for solvent exchange (12 hrs immersion) to obtain cellulose hydrogel

fibers. The hydrogel fibers were subjected to solvent exchange in tert-butanol for 30 min, and followed by freeze-drying to produce cellulose aerogel fibers.

Preparation of PEI aerogel fibers via chemical crosslinking (CE/GA/PEI-aerogel fiber)

Cotton fibers (0.28 g) were dissolved in a mixed solution of 1.6 g ILs and 6.4 g DMSO under magnetic stirring at 45 °C until complete dissolution was achieved. The spinning solution was extruded from a pump-controlled syringe into a water bath. Subsequently, the hydrogel fibers were immersed in an 8% NaOH solution at 5 °C for 5 hrs. After washing, 30 mL of 2.7% PEI solution was added dropwise, and the mixture was stirred at 50 °C for 3 hrs. Upon cooling to room temperature, 1 mL of glutaraldehyde was added, followed by stirring for 2 hrs. The fibers were then filtered and repeatedly washed with water. The obtained hydrogel fibers were subjected to solvent exchange in tert-butanol for 30 min, and followed by freeze-drying. The as-prepared fibers were then immersed in a responsive dye solution, and a secondary freeze-drying step was performed to obtain the final cellulose aerogel fibers.

Preparation of crosslinked PEI aerogel fiber (CE@PEI-aerogel fiber)

CE@PEI fibers (0.28 g) were dissolved in a mixed solution consisting of 1.6 g ILs and 6.4 g of DMSO, followed by magnetic stirring at 45 °C until complete dissolution of the fibers. The spinning solution was then extruded into a coagulation bath containing reactive dye aqueous solution. The obtained hydrogel fibers were immersed in a reactive dye solution for another 12 hrs, then placed in tert-butanol bath for 30 min, which was followed by freeze-drying to produce the final CE@PEI-aerogel fiber.

Characterization

The microstructures of aerogel fibers were observed using a scanning electron microscope (JEOL-7800F, JEOL Ltd., Japan). The chemical composition and cross-linking reactions of the

modified aerogel fibers were comprehensively analyzed using Fourier-transform infrared spectroscopy (Nicolet IS50, Thermo Fisher Scientific, USA) and X-ray photoelectron spectroscopy (ESCALAB 250XI, Thermo Fisher Scientific, USA). Crystallinity was investigated using an X-ray diffractometer (Empyrean, PANalytical, Netherlands) with Cu-Kα radiation, within a 2θ range of 10° to 40°. The mechanical properties of the fibers were evaluated using a fiber tensile testing machine (XQ-1AN, Shanghai New Fiber Instrument Co., Ltd., China) with a gauge length of 2 cm and a testing speed of 10 mm/min. To ensure statistical reliability, at least five samples (5 cm in length) were tested under each condition. The absorbance of the dye solution was measured at λ_{max} using a UV-Vis spectrophotometer (UV-3600, Shimadzu, Japan) to evaluate the dye uptake rate. In the thermal insulation performance test, fabrics of identical area and thickness were placed on a heating stage under identical conditions. Thermocouples were subsequently attached to the fabric surfaces to record temperature variations. An infrared thermal imager (HM-TPH103-3AQF, Hangzhou Microimage) was employed for imaging to visually demonstrate the surface temperature distribution of the test specimens.

Gas response test

The gas detection system comprises a gas circulation pump, a sample chamber, and an infrared spectrometer. Initially, the prepared sample is placed into the sample chamber and hermetically sealed. Subsequently, a precise volume of the target gas is injected into the gas pump using a microsyringe, where it undergoes rapid vaporization and circulates within the odor detection system. Through the measurement of time-resolved infrared absorption intensity at specific wavelengths, quantitative analysis of gas concentration within the detection system is conducted.

Quantitative assessment of color variation intensity

A smartphone (iPhone 14) was used to capture sample images under fixed distance conditions (15 cm). The chromatic variations in the images were quantitatively analyzed using Adobe Photoshop software, with color changes evaluated based on the L*a*b* color space system established by the International Commission on Illumination (CIE). This color space model is designed to simulate the human visual perception of color, comprising three components: L* represents the luminance parameter, a* reflects the hue variation range from green to red, and b* indicates the hue shift from blue to yellow. The CIELab system was selected for color quantification analysis due to its linear perceptual characteristics, where the color difference (dE) between two colors can be determined by calculating the Euclidean distance between their respective color coordinates. Assuming the coordinates of two colors are (L_1*, a_1*, b_1*) and (L_2*, a_2*, b_2*), the quantitative color difference can be calculated using the following formula:

$$E = \sqrt{\left(L_2^* - L_1^*\right)^2 + \left(a_2^* - a_1^*\right)^2 + \left(b_2^* - b_1^*\right)^2} \quad (1)$$

Human eye can distinguish the difference between two colors when the dE value is greater than 3.3.

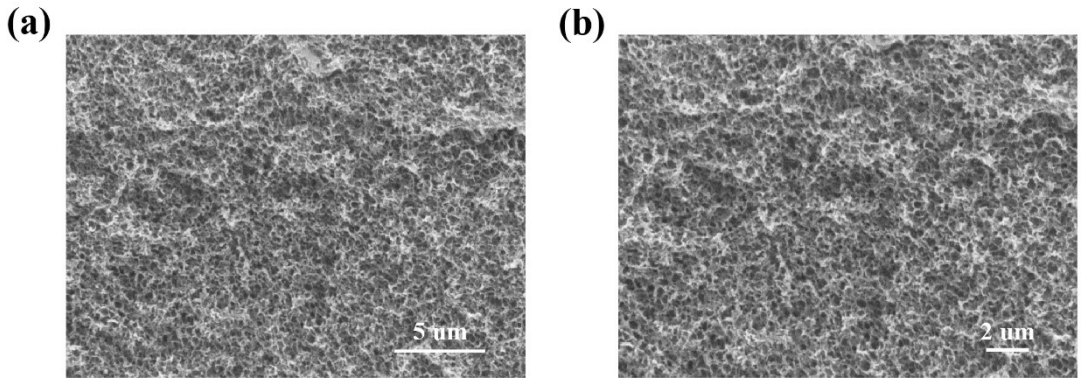

Figure S1 SEM image of CE@PEI-aerogel fibers.

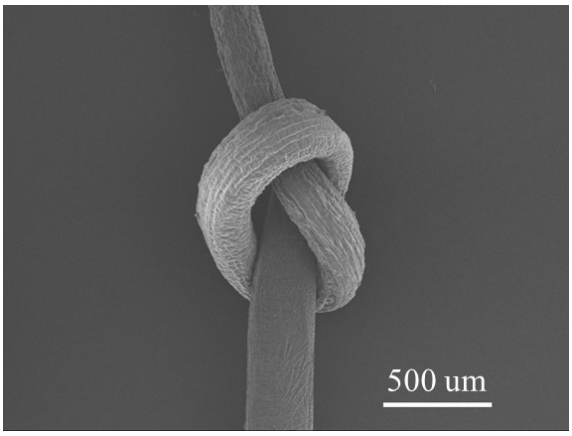

Figure S2 SEM image of knotted CE@PEI-aerogel fiber.

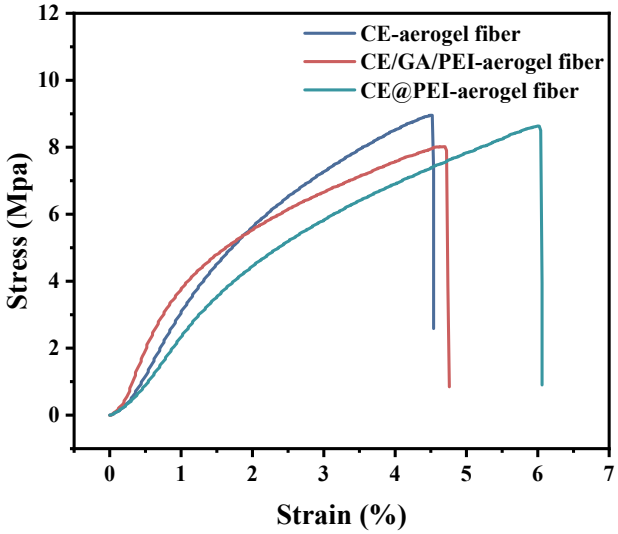

Figure S3 Stress-strain of CE-aerogel fiber, CE/GA/PEI-aerogel fiber and CE@PEI-aerogel fiber.

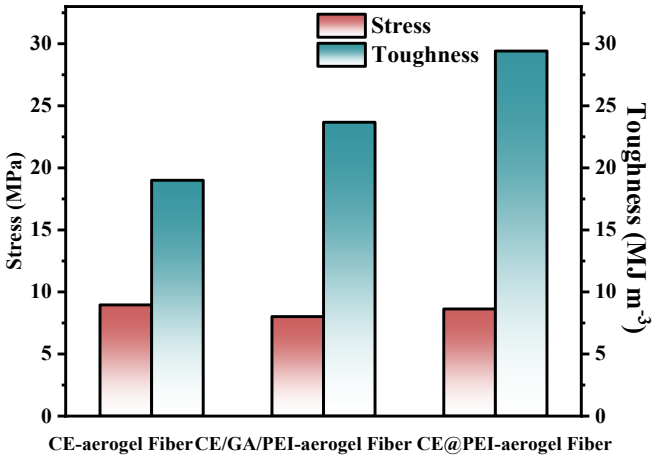

Figure S4 Tensile strength and toughness of CE-aerogel fiber, CE/GA/PEI-aerogel fiber and CE@PEI-aerogel fiber.

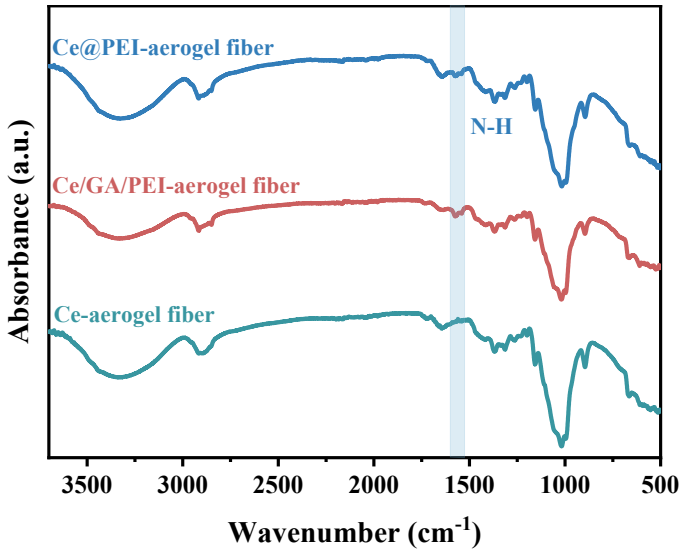

Figure S5 FT-IR spectra of CE-aerogel fiber, CE/GA/PEI-aerogel fiber and CE@PEI-aerogel fiber.

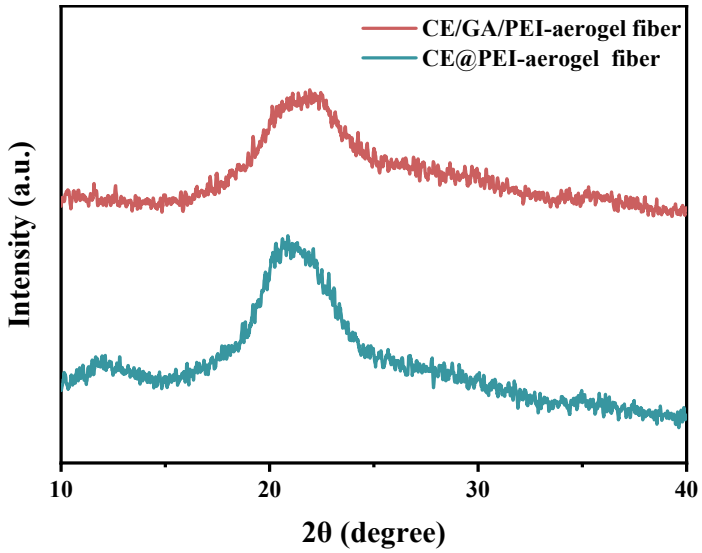

Figure S6 XRD curves of CE-aerogel fiber, CE/GA/PEI-aerogel fiber and CE@PEI-aerogel fiber.

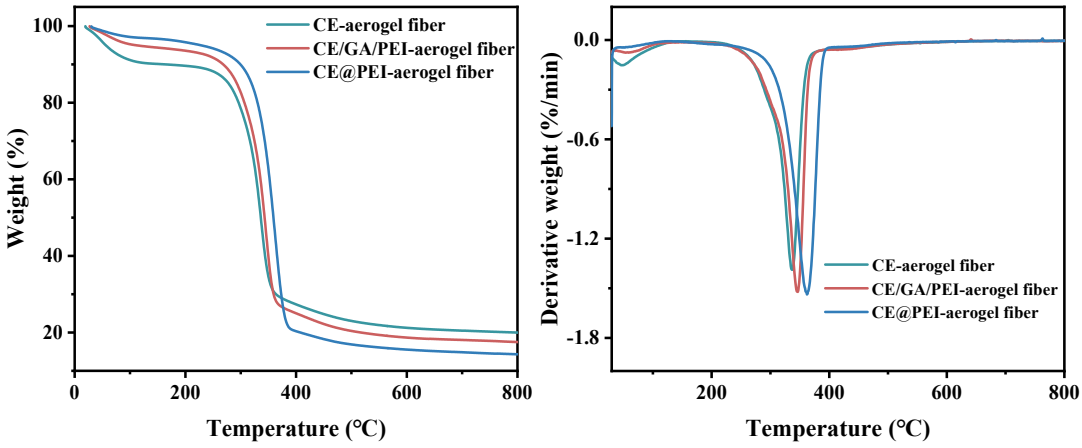

Figure S7 TGA and DTG results of CE-aerogel fiber, CE/GA/PEI-aerogel fiber and CE@PEI-aerogel fiber.

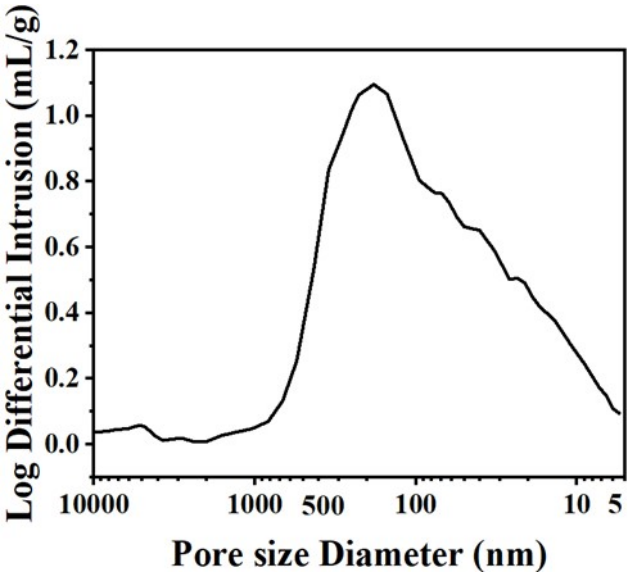

Figure S8 The differential mercury adsorption volume - pore size curve of CE@PCE@PEI aerogel fibers.

In the range of 3200–3500 cm^{-1} (N–H/O–H stretching region), the dyed fibers exhibit enhanced peak intensity. This is attributed to the overlapping N–H/O–H signals from both the reactive red dye and the fiber functional groups, as well as signal amplification due to hydrogen bonding between polar groups such as the sulfonate groups of the dye and the fiber matrix. The peak near 1600 cm^{-1} becomes sharper, resulting from the superposition of the azo group (–N=N–) stretching vibration of reactive red and the inherent fiber signals. The peak between 1200 and 1000 cm^{-1} showed increased intensity. This change arises from the overlap of the S=O stretching vibration of the dye sulfonate group with the C–O–C peak of the fiber, along with the enhanced stretching vibration of the C–N covalent bond formed via nucleophilic substitution.[3] A new peak emerges in the 800–850 cm^{-1} range, corresponding to the skeletal vibration of the triazine ring in the reactive red dye. Collectively, these infrared characteristic peaks confirm the occurrence of nucleophilic substitution between the $–NH_2$ groups of PEI and the triazine ring of the dye.

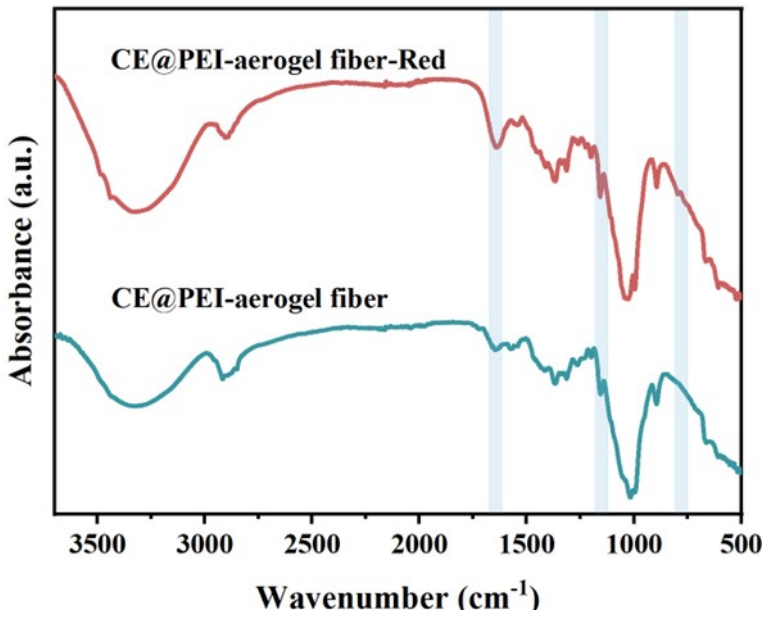

Figure S9 FT-IR spectra of CE@PEI-aerogel fibers dyed with reactive red dyes and undyed CE@PEI-aerogel fibers.

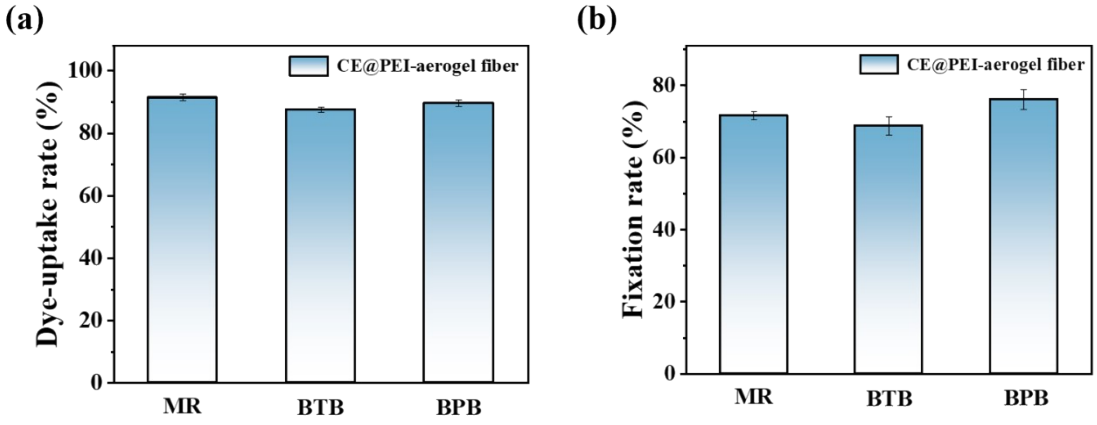

Figure S10 Dye-uptake rate and color fixation rate of CE@PEI-aerogel fibers for MR, BTB, and BPB dyes.

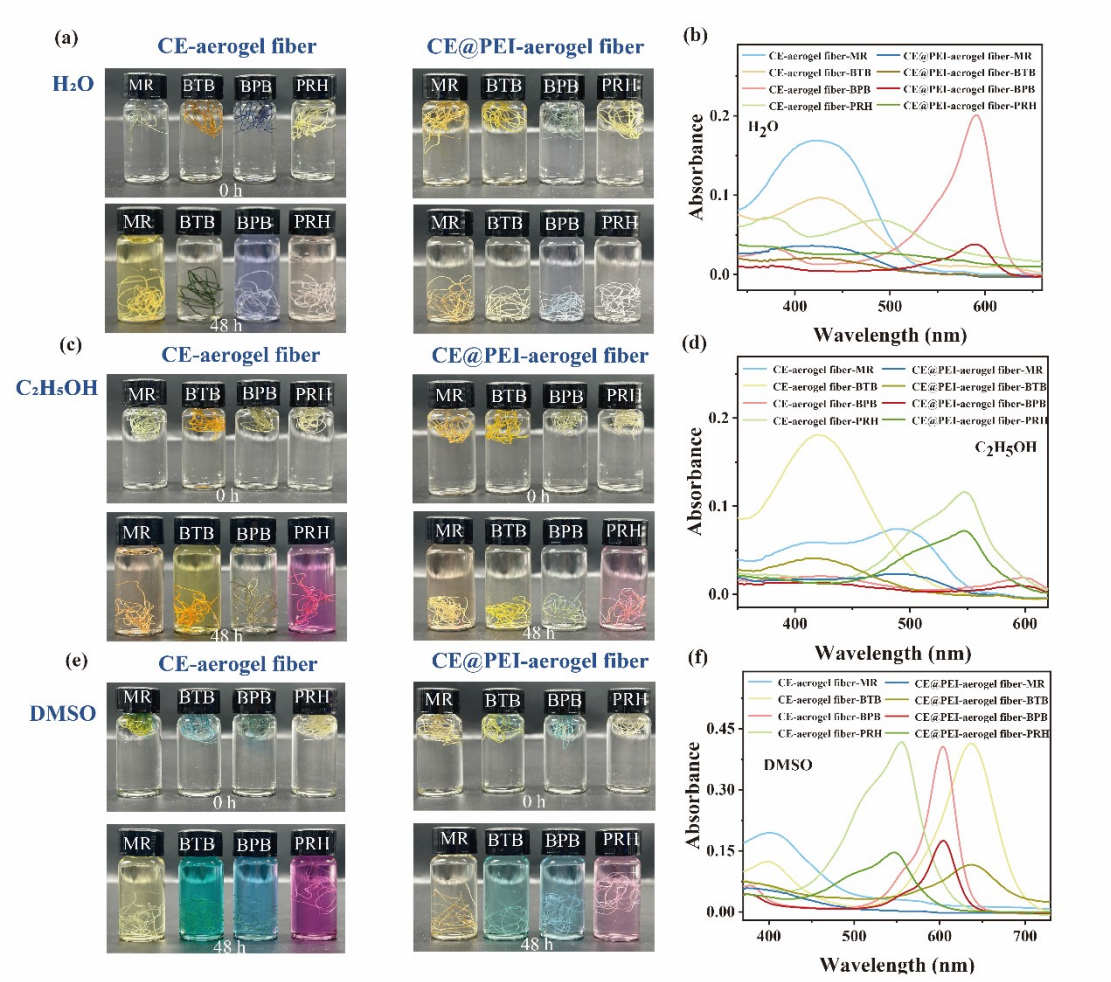

160

161 **Figure S11** Fading conditions and ultraviolet spectral diagrams of CE-aerogel fibers

162 and CE@PEI-aerogel fibers in water, alcohol, and DMSO systems.

163

164

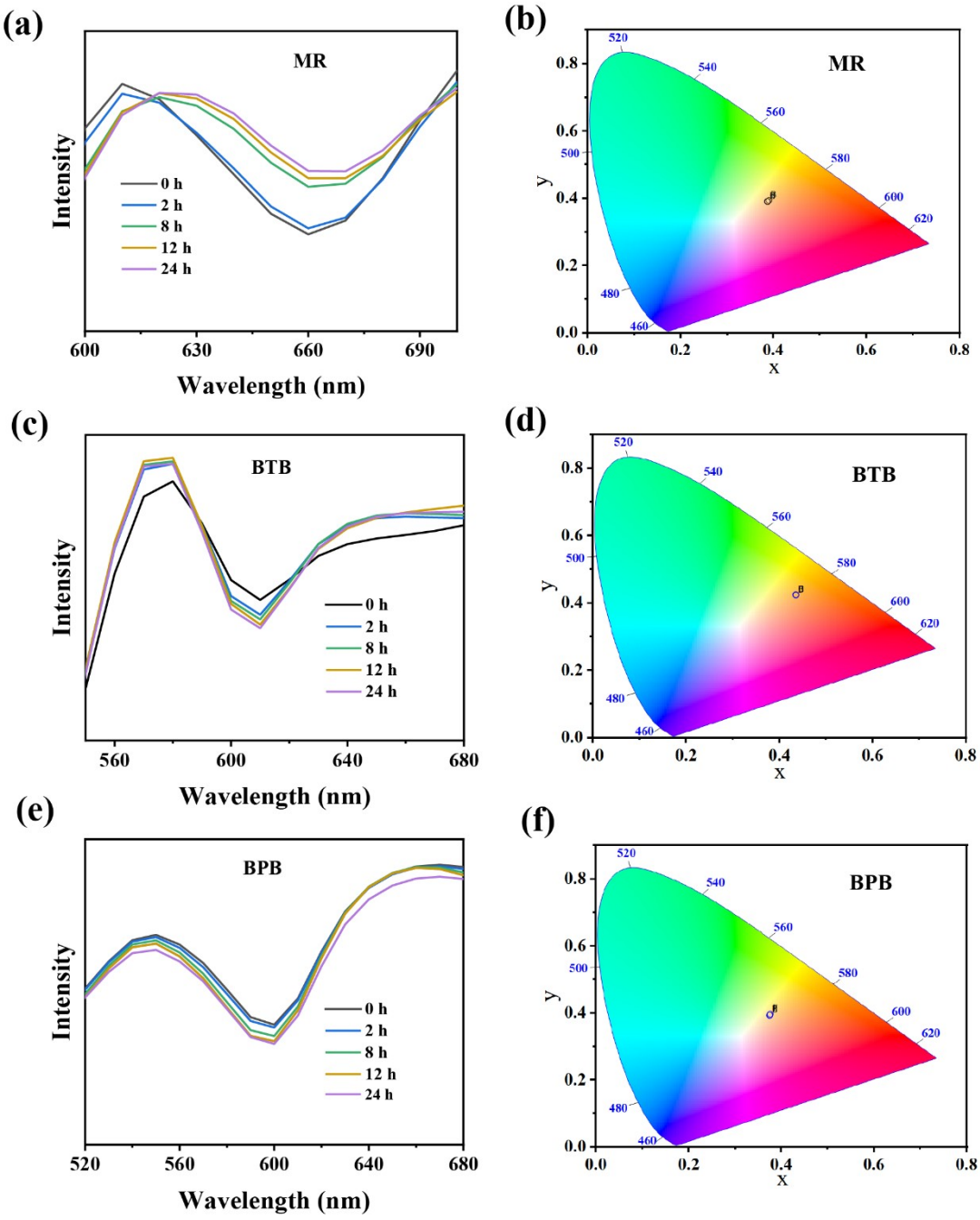

165

166 **Figure S12** Spectral intensity and CIE color coordinate diagrams of CE@PEI-aerogel

167 fibers in (a-b) MR dye, (c-d) BTB dye, and (e-f) BPB dye.

168

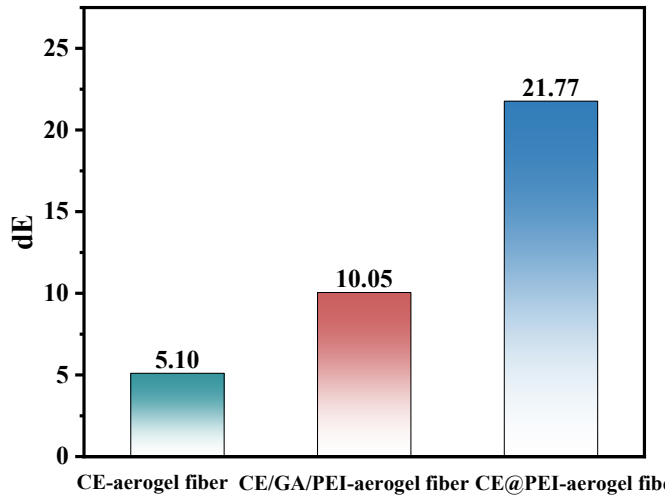

Figure S13 Saturated dE values of CE-aerogel fiber, CE/GA/PEI -aerogel fiber and CE@PEI -aerogel fiber at 100 ppm acetic acid concentration.

Figure S14 Methyl red discolouration mechanism.

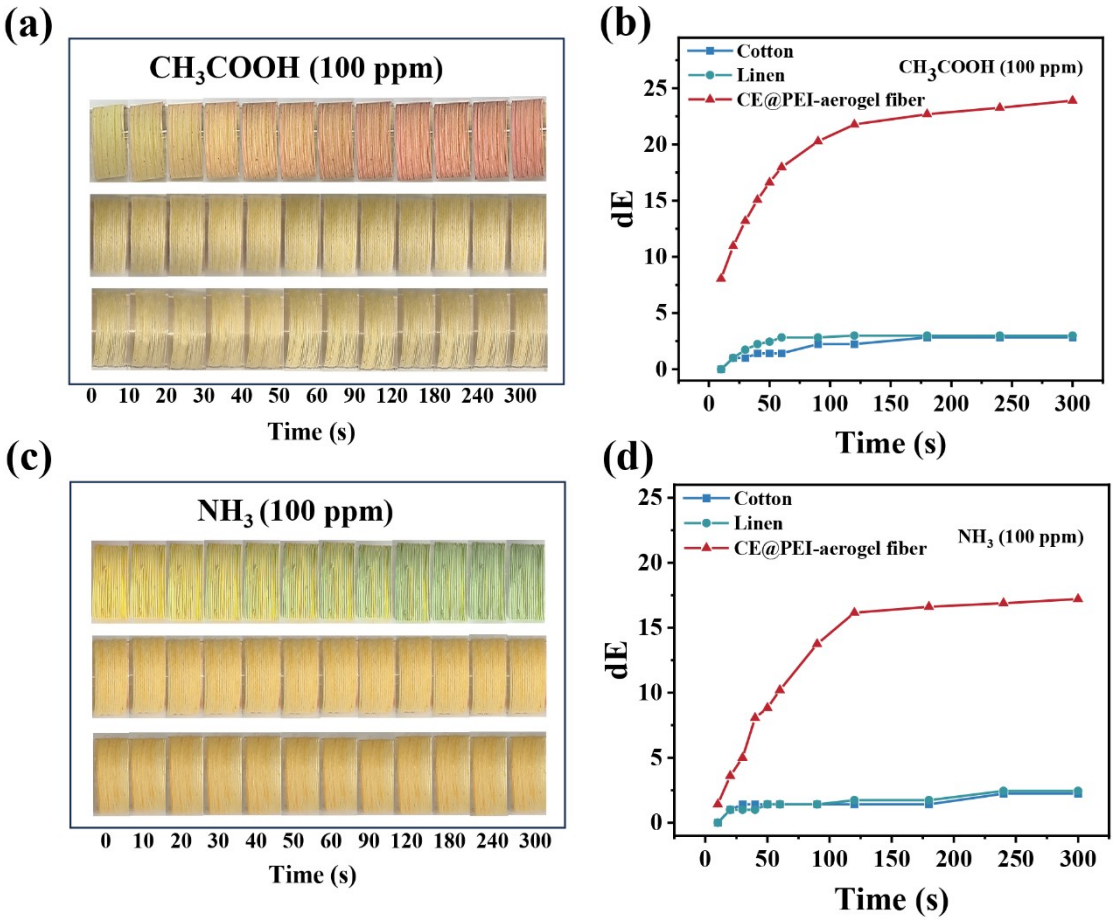

Figure S15 (a) Color changes of CE@PEI-aerogel fibers, cotton fibers, and flax fibers in a 100 ppm acetic acid environment. (b) Changes in the dE values of three types of aerogel fibers in a 100 ppm acetic acid environment. (c) Color changes of CE@PEI-aerogel fibers, cotton fibers, and flax fibers in a 100 ppm ammonia environment. (d) Changes in the dE values of three types of aerogel fibers in a 100 ppm acetic acid environment.

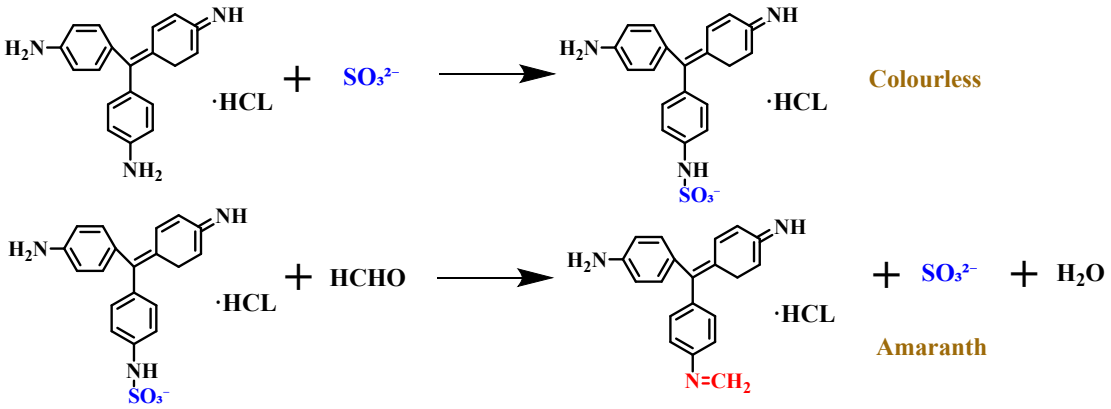

Figure S16 Reaction mechanism of the Schiff reagent system for the detection of formaldehyde, constructed by combining hypromellose hydrochloride and sodium sulphite.

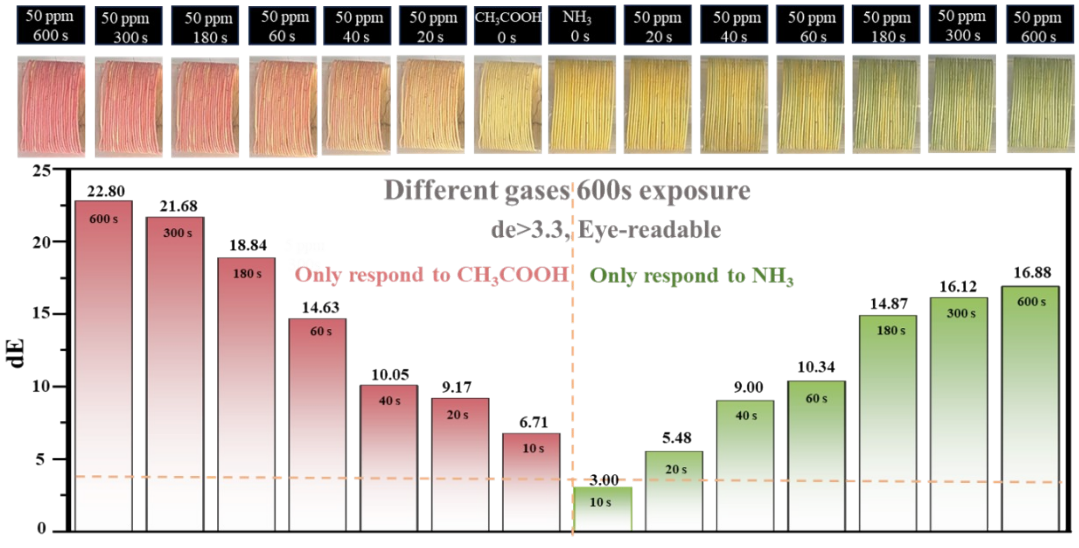

Figure S17 Color changes and dE values of CE@PEI-aerogel fibers in response to specific gases in a mixed gas system.

To investigate the impact of the introduction of PEI and dyes on the nanoporous structure and thermal properties of the aerogel fibers, we conducted further characterization and data analysis using SEM, thermal conductivity measurements(Table S3), and TGA/DTG(Figure S7).

Without PEI and dyes, the aerogel fibers exhibited large pores with a size of 1-3 μm (Figure S18a). This microstructure facilitated convective heat transfer and allowed close contact between fiber molecular chains, corresponding to a thermal conductivity of 0.419 mW/(m·K). Meanwhile, the presence of micron-sized pores accelerated heat conduction, while weak hydrogen bonds could not effectively restrict the thermal motion of cellulose chains, leading to a a relatively low initial decomposition temperature in TGA/DTG.

After grafting PEI grafting and subsequent dyeing, SEM results reveal a uniform nanoporous structure with pore sizes ranging from 5 to 400 nm (Figure S18b). This nanoporous structure restricts air molecule convection, lowering the thermal conductivity to 0.296 mW/(m·K). Simultaneously, the physical barrier of the nano-micropores slows heat transfer, and enhanced intermolecular interactions better constrains the molecular chain. As a result, the initial decomposition temperature is elevated to 360°C in TGA/DTG. We propose that hydrogen-bond between PEI and cellulose slows the solvent–coagulant exchange rate, suppressing the formation of large-pores.

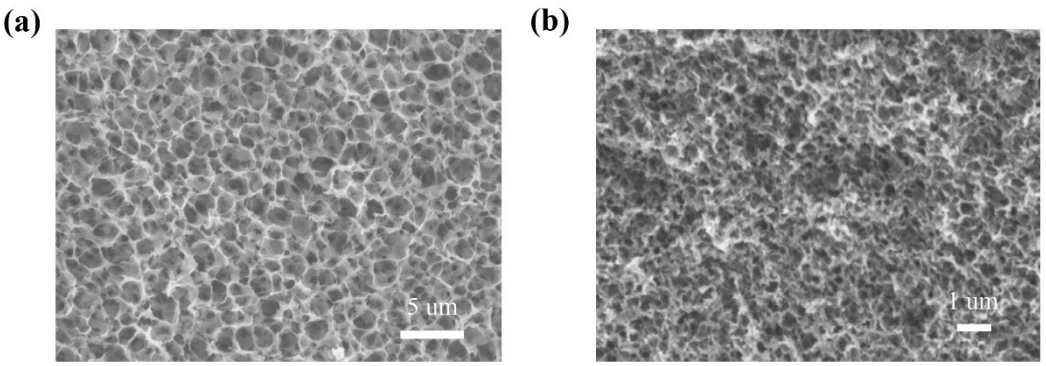

Figure S18 SEM images of (a) CE-aerogel fibers and (b) CE@PEI-aerogel fibers.

Table S1 Thickness and thermal conductivity of different textiles.

Material	Thickness (mm)	$T_{surface}$ (°C)	λ(mW/m·K) Measured by steady-state device
Nylon	0.73±0.01	49.1	118.7±1.6
Polyester	0.76±0.02	48.9	93.7±2.5
Linen	0.6±0.05	48.5	66.0±5.5
Cotton	0.76±0.02	47.3	49.8±1.8
CE@PEI-fiber	0.78±0.02	42.8	29.5±0.8

Table S2 The pore structure parameters of CE@PEI aerogel fiber.

Porosity (%)	volume density (g/ml)	Apparent (framework) density (g/ml)	average pore size 4V/A (g/ml)	Median pore diameter V (g/ml)	Median pore diameter A (g/ml)	Total pore volume (g/ml)	Total pore area (g/ml)
66.55	0.42	1.26	56.79	152.62	20.04	1.58	110.98

Table S3 CE-aerogel fibers, CE@PEI-aerogel fibers, optical and infrared images and thermal conductivity on a heating platform at 30-100 °C.

sample	Stage temperature				λ(mW/m·K)
	30 °C	60 °C	80 °C	100 °C	
CE-aerogel Fiber	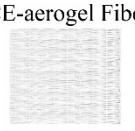	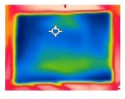	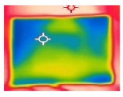	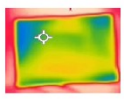	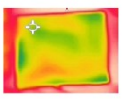	29.5±0.8
CE@PEI-acroge Fiber			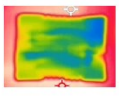	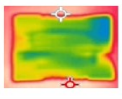	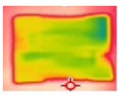	41.9±2.1